

3D geophysical imaging to study the evolution of a debris covered glacier in the Dolomites (South-Eastern Italian Alps)

ZANONER T.(1), FRANCESE R.(2), BONDESAN A.(1), GIORGI M.(2), CARTON A.(1), SEPPI R.(3), NINFO A.(1), ZUMIANI M. (4)

(1) University of Padova - Department of Geosciences, PADOVA, ITALY; (2) National Institute of Oceanography and Experimental Geophysics (OGS), TRIESTE, ITALY; (3) University of Pavia - Department of Earth and Environmental Sciences, PAVIA, ITALY; (4) Geological Survey - Autonomous Province of Trento, TRENTO, ITALY

INTRODUCTION

The glaciers of the Dolomites are mostly small and hosted in cirques. Most of them were progressively covered by large amount of debris throughout the retreating phase occurred after the Little Ice Age (LIA), allowing their preservation even at relatively low altitudes. The internal structure of the ice-debris mass and the morphology of the bedrock of the Cima Uomo Glacier were investigated using a 3D resistivity imaging and 2D radar profiling. Field data were collected with 48-electrode Syscal R1 Georesistivimeter and with a GSSI SIR-2000 radar system equipped with an unshielded 75 MHz antenna. Both a pole-dipole, using 6 remote poles, and Wenner mode was adopted (fig. 10).

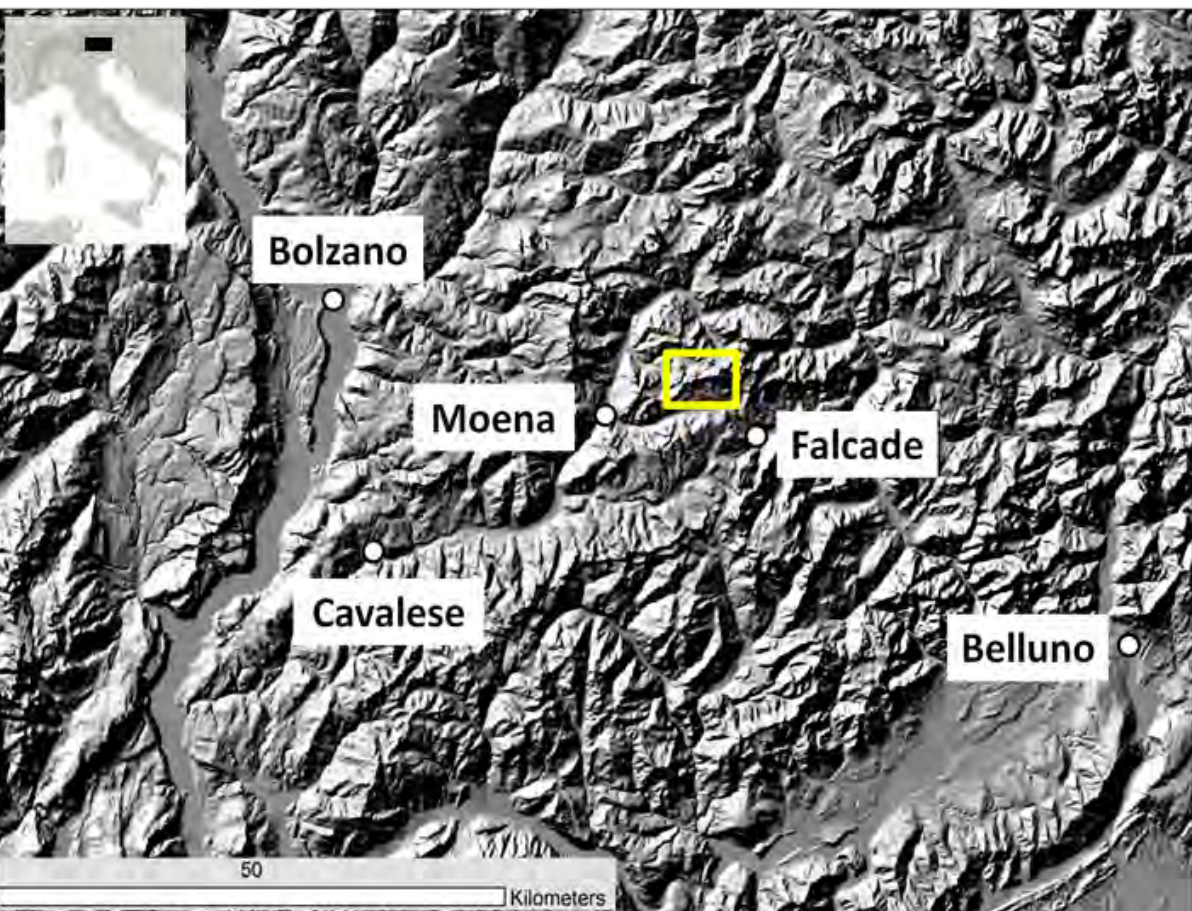


Fig. 1 – Location of the study area.

STUDY SITE

The Cima Uomo glacier is located in upper Val San Nicolò (Dolomites, Trentino, Fig. 1) between 2400 and 2600 m of altitude. It is a cirque glacier, mainly fed by avalanches and now completely covered by a thick layer of debris. The surface morphology suggests that the glacial system currently consists of two separate ice masses. This glacier has been reported in several historical maps, where its evolution from clean to debris-covered glacier can be observed (Carton et al., 2009).

GEOMORPHOLOGICAL OBSERVATIONS

A well-defined morainic ridge marks the maximum extension of the glacier at the LIA. On the south-west part, the arch is more advanced and closes the valley, reaching a small rounded relief. The north-eastern moraine has a S-shape and his higher portion marks a less advanced sector of the glacier. On the more advanced lobe, several transverse ridges and furrows are visible, suggesting that the glacial debris is still in motion

COMPLEMENTARY RESEARCH

BTS and GST measurements

The evolution of Cima Uomo ice-debris mass is probably driven by permafrost conditions, and, in order to detect the presence of permafrost in this site, BTS measurements were carried out in late winter 2009, 2010 and 2011. In addition, 8 data loggers for continuous GST measurements were placed at different elevations and on different morphological units in autumn 2009. As suggested by the low temperature of the ground observed with the two applied methods, permafrost conditions are largely present in the debris body.

Solar radiation

A specific investigation was carried out on the solar radiation of the study area, in order to spatially quantify how this factor interacts in the evolution of Cima Uomo glacier. The topographic solar radiation was calculated in GIS using a DEM (cell size of 2 m) derived from a LIDAR survey carried out by the Autonomous Province of Trento between 2006 and 2008 (fig. 2).

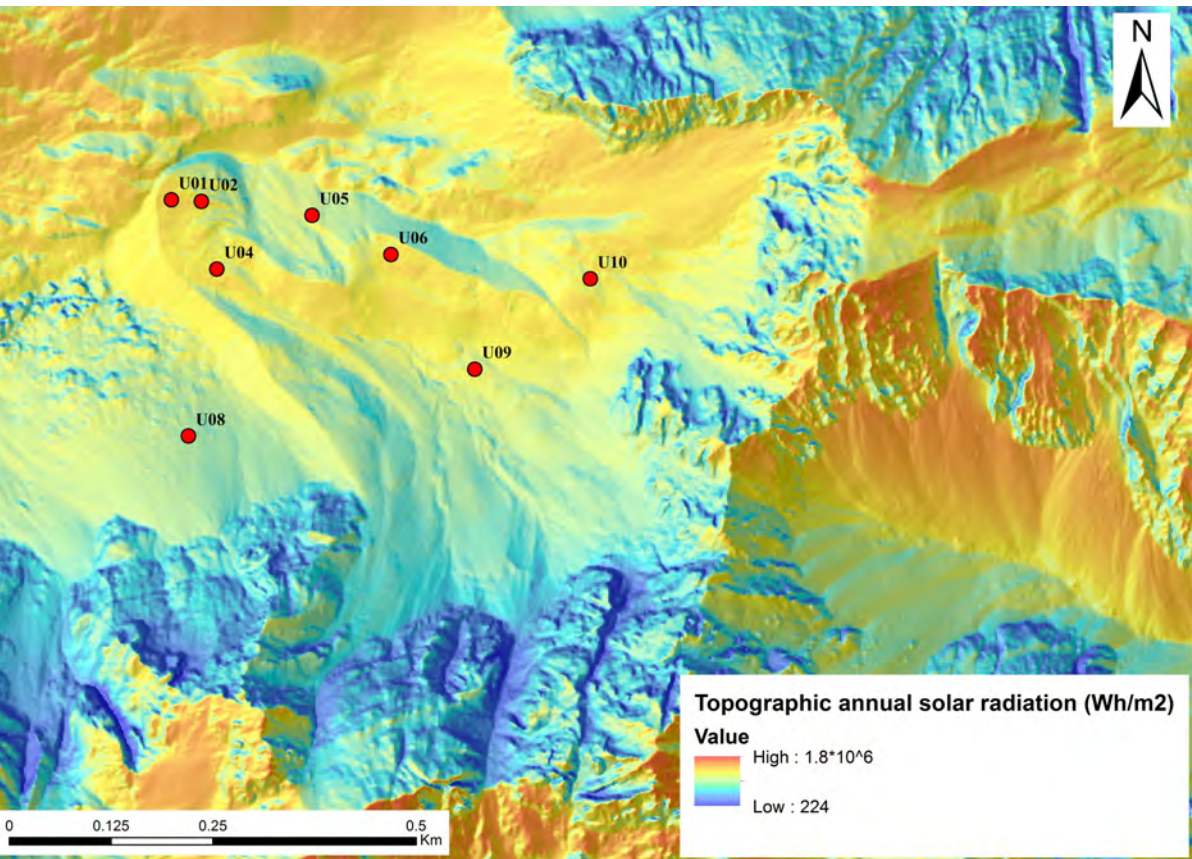


Fig. 2 – Topographic annual solar radiation draped over a hillshade of study area. The red dots indicate the location of the thermometric probes.

Topographical measures

A topographical monitoring net has been set in order to measure both the average annual horizontal and vertical displacement of the Uomo glacier. A total of 14 surveying points have been positioned on boulders aligned along three parallel lines at different distance from the front (fig. 3). The main horizontal velocity field shows higher values along the central longitudinal axis of the glacier. Values range from 22 cm/a in the up-valley central portion, to 8 cm/a in the left outer flank. Vertical lowering is mainly due to ice melting.

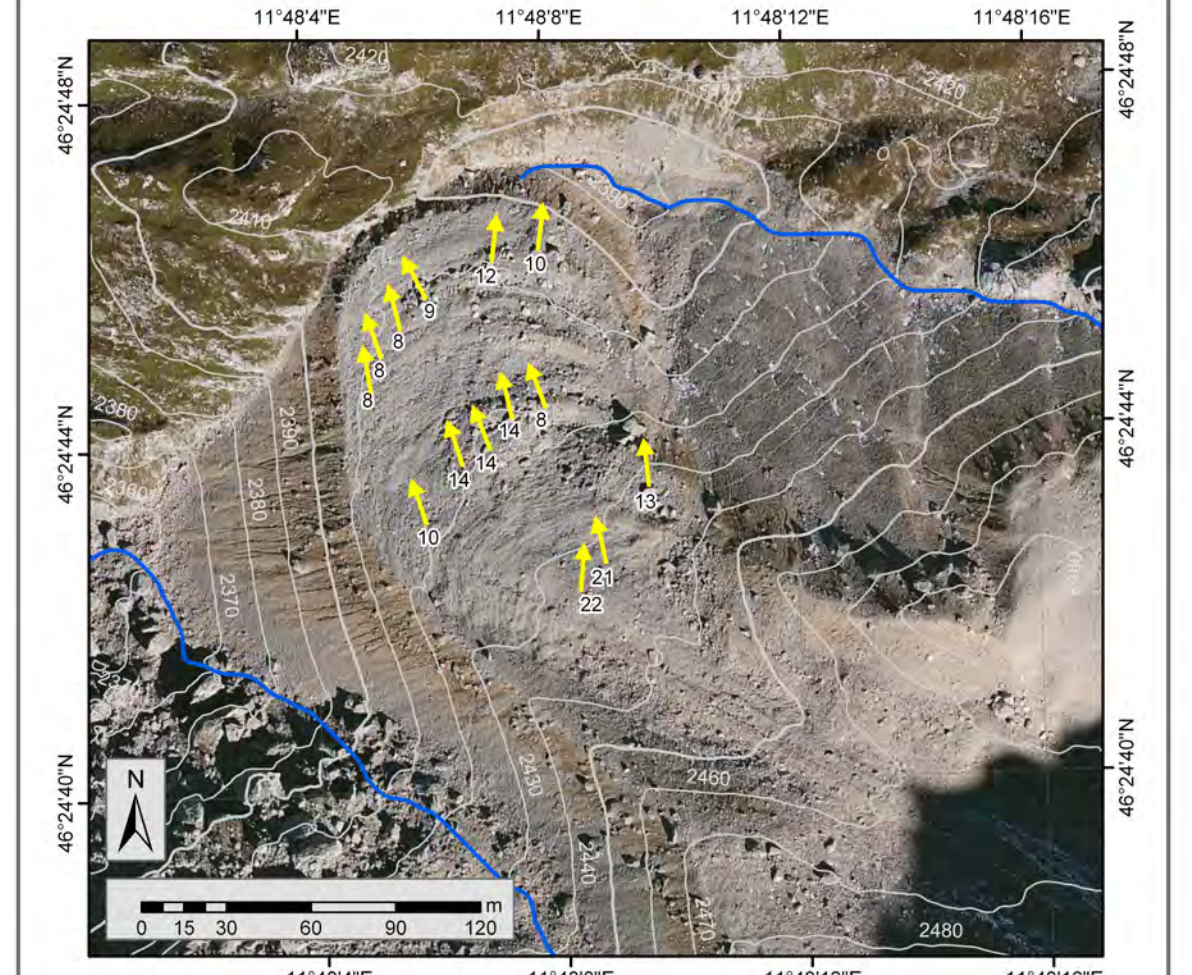
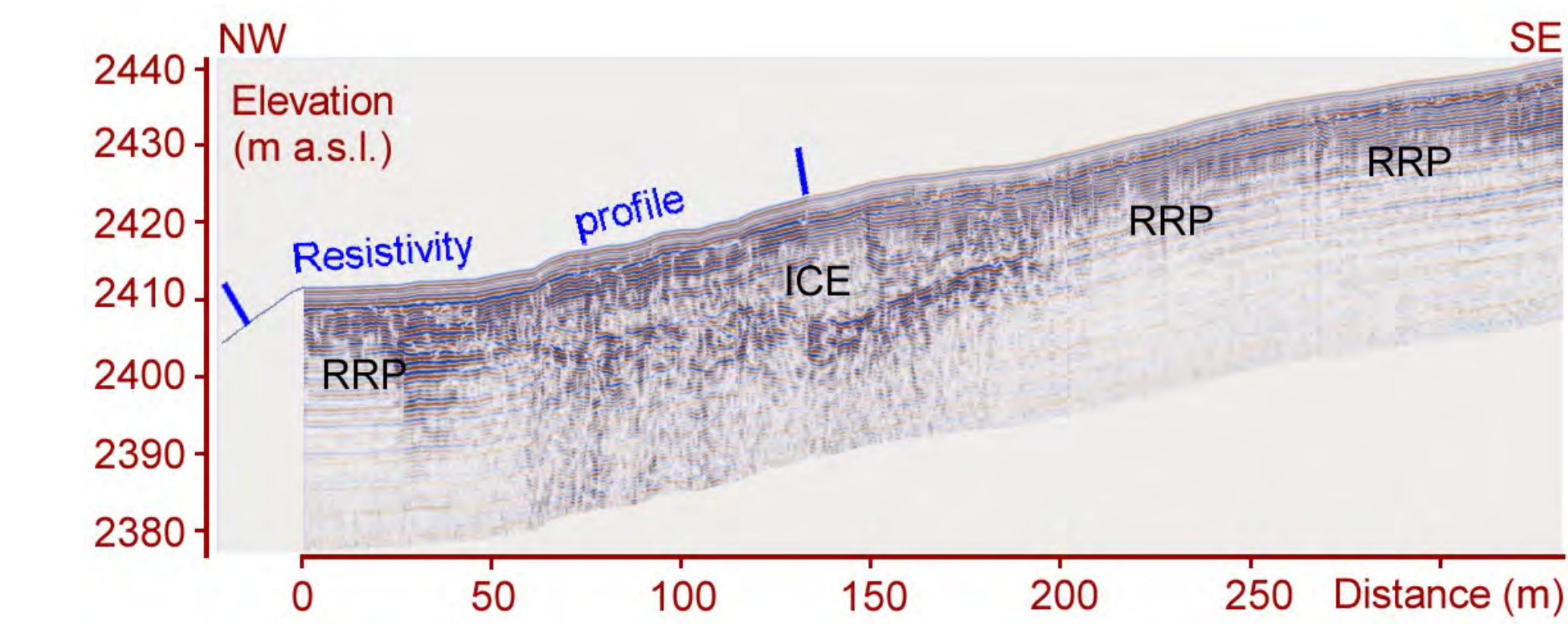


Fig. 3 – Annual average horizontal velocity. Legend: yellow arrows: velocity vectors: cm/a; grey lines: contours in m a.s.l.; blue lines: ephemeral water stream

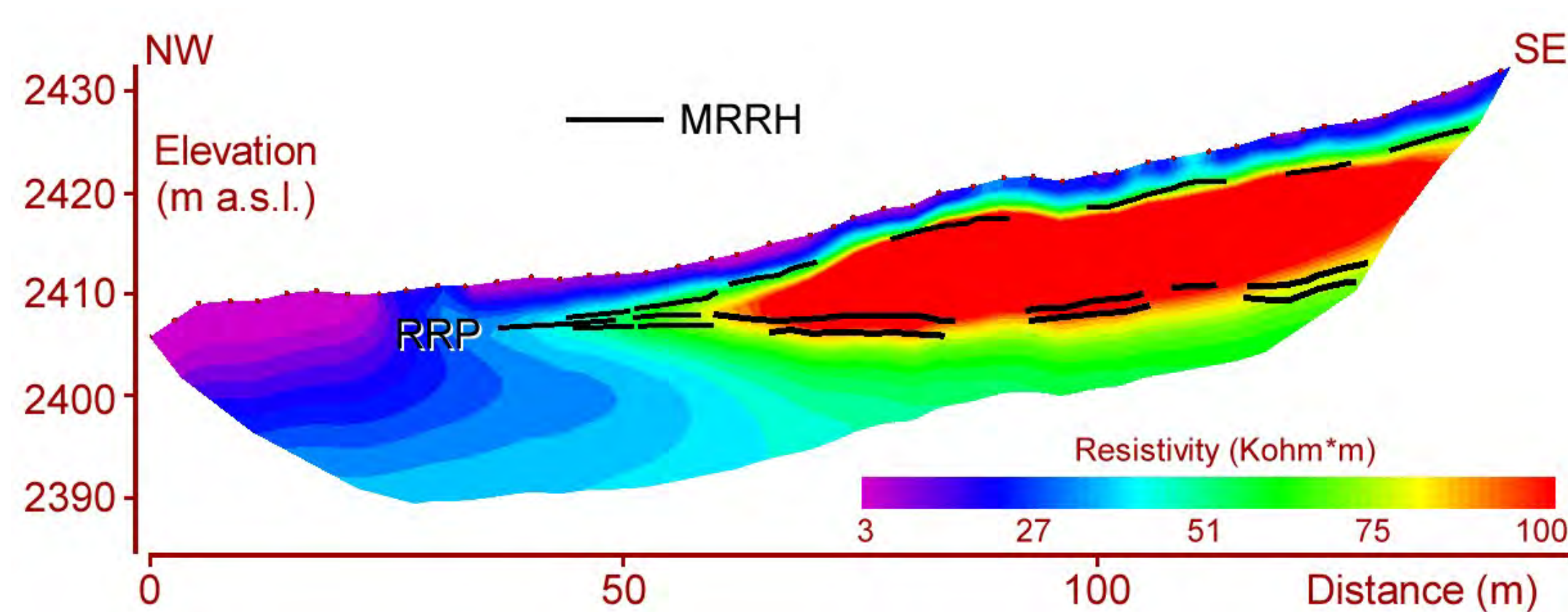


GPR SURVEY

The radar signature superimposed on the ERT profile (Major Radar Reflecting Horizons - MRRH in fig. 4) shows the close correspondence between the resistivity distribution in the subsurface and the radar reflections. This radar marker also indicates, with a large degree of confidence, how the resistivity value of 80 Kohm*m represents the threshold between the debris and the ice body. The thickness of the ice body at the horizontal distance of 100 m along the profile is about 10 m.

Fig. 4 – GPR profile. RRP: Radar reduced penetration zone.

Fig. 5 – Resistivity profile. MRRH: Major radar reflecting horizons. RRP: Radar reduced penetration zone.



2D ERT SURVEY

The resistivity in the 2D ERT profile ranges from 3 Kohm*m to values larger than 100 Kohm*m. The image (fig. 5) shows a highly resistive unit (with values of several hundreds of Kohms*m). This resistive unit pinches out moving northwestward and the values are compatible with a buried ice body (Leopold et al., 2011).

GEOPHYSICAL SURVEY, DATA ACQUISITION AND PROCESSING

The geophysical survey was focused on assessing the presence of ice in the subsurface and measuring its geometry. Radar measurements were carried out using a GSSI SIR 2000 system equipped with a 70 MHz antenna while resistivity data were collected with a 48-electrode IRIS Syscal R1 georesistivimeter.

Resistivity data were inverted using the software package ERTLAB 3D. The GPR signature of the buried deposits appears to be very sharp in the distance interval comprised between 50 m and 200 m (fig. 4) while along the other segments of the profile the reflectivity is fairly low. The radar wave is attenuated in the first segment of the profile (0-50 m) probably because of the absence of ice in the sediments. The radar wave is also severely attenuated in the middle and in the last segments of the profile where there is direct evidence of the presence of ice. This last occurrence is caused by the existence of an uppermost conductive layer comprised of silts and clays that reduces the signal penetration (RRP zones in fig. 4). The dipping and concave reflecting horizon, clearly visible in the mid portion of the profile, probably bounds a thin ice body. The bottom of the ice body is located at an elevation of approximately 2400-2410 m while its top appears to be very close to the surface.

The terminal moraine (distance interval 0-25 m) exhibits resistivity values in the order of 3 to 5 Kohm*m. The resistivity of these deposits appears to be very high although a silty-sand matrix is clearly visible on the surface and it's probably caused by the presence of large voids and cavities in depth. The covering debris show resistivity values comparable to the ones of the terminal moraine although slightly higher. The thickness of this coverage layer is somewhat regular and it results of approximately 2 m. A better image of the geometry of the buried ice body is visible in the 3D ERT volume (figg. 6, 7 and 9). The resistivity in the surveyed volume ranges from 3 Kohm*m to several hundreds of Kohm*m. The terminal moraine (Figure 9 in the middle) exhibits the lowest resistivity values and clearly bounds a highly resistive ice body. The ice in the subsurface could be better evidenced using the threshold value of 80 Kohm*m (Figure 9 in the left) as defined by the joint analysis of GPR and ERT data. The ice body geometry is somewhat complicated and it appears as an ensemble of several lobes with a maximum thickness of 15 m in the central portion of the ice body.

The projected surface of the ice body, in the area covered by the 3D ERT, is about 4650 square meters while the volume could be estimated in approximately 23000 cubic meters.

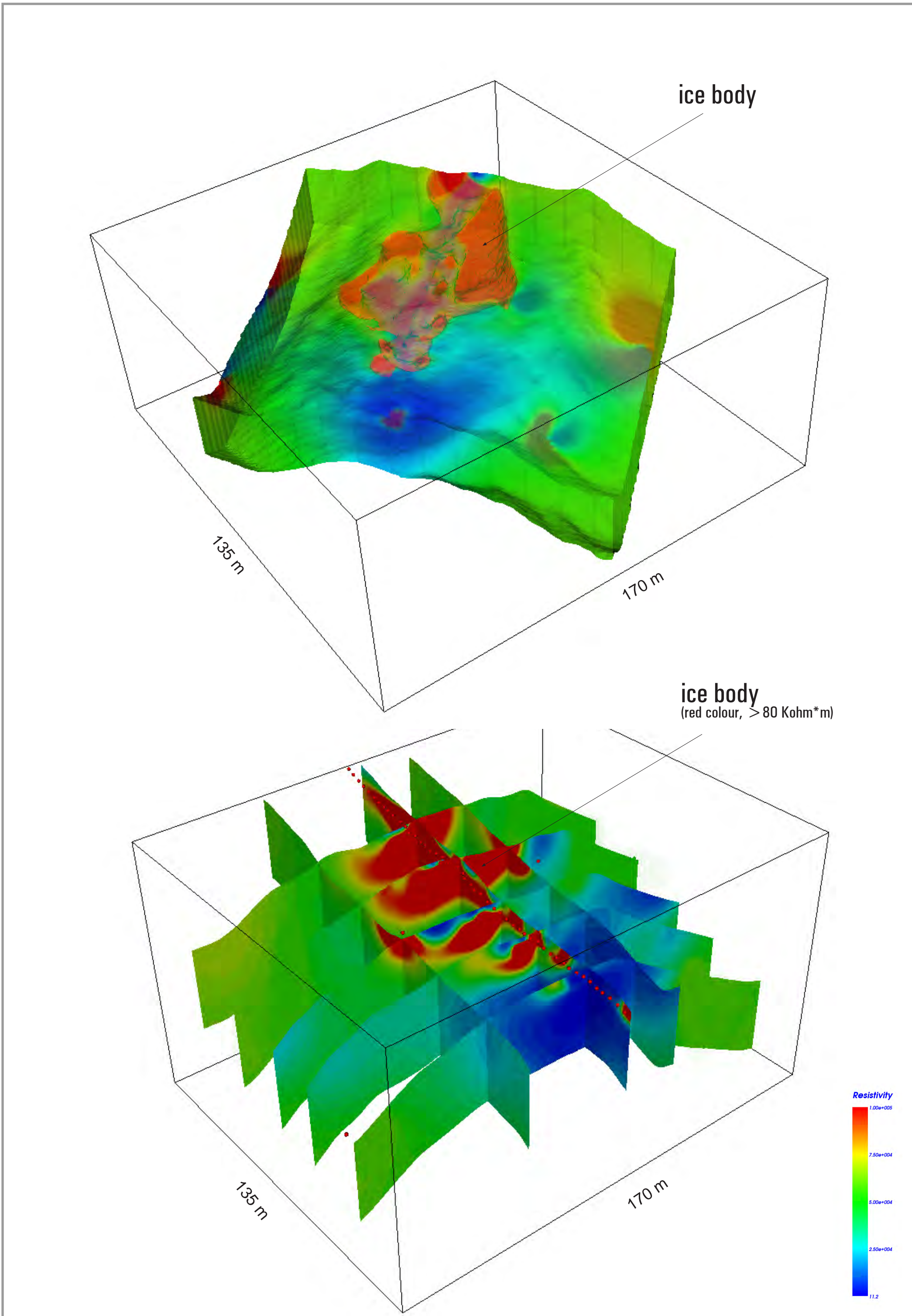


Fig. 6 – Resistivity volumes with cross sections.

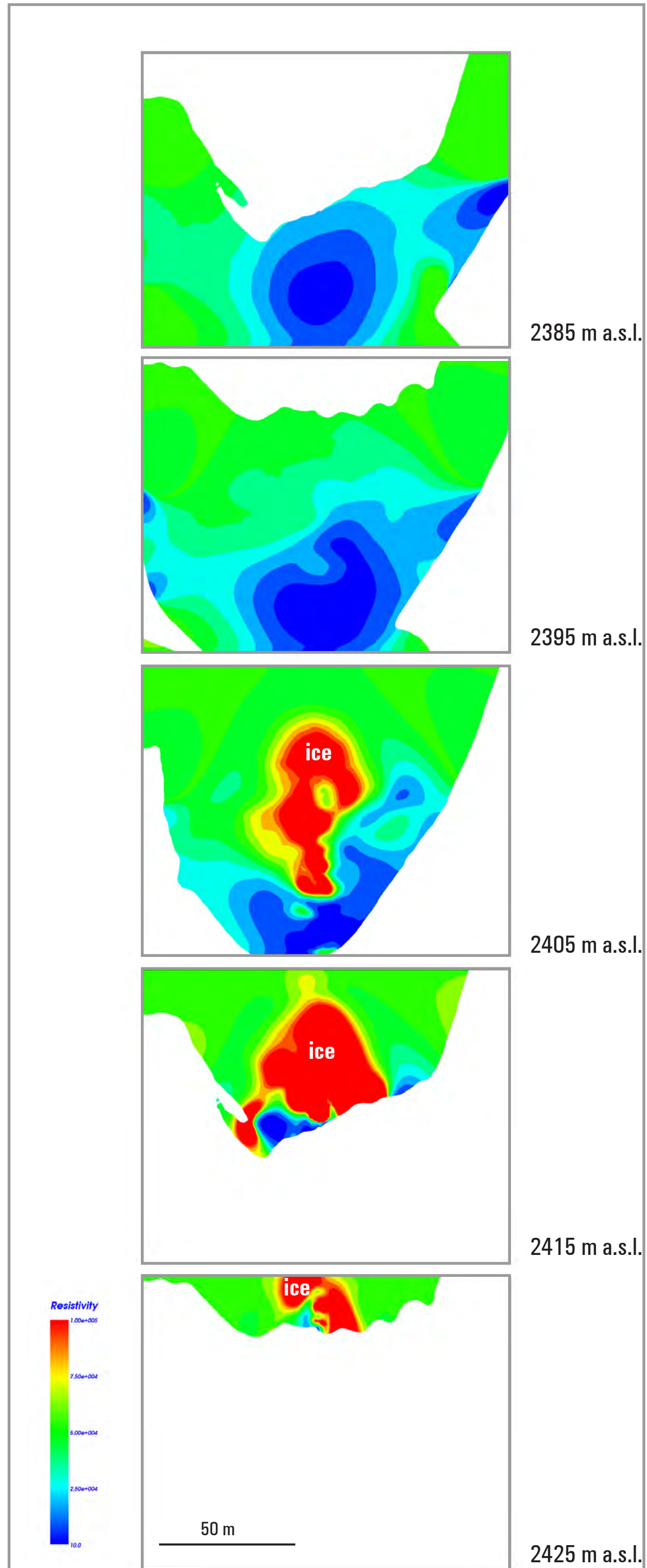


Fig. 7 – Resistivity tomography (horizontal planes).

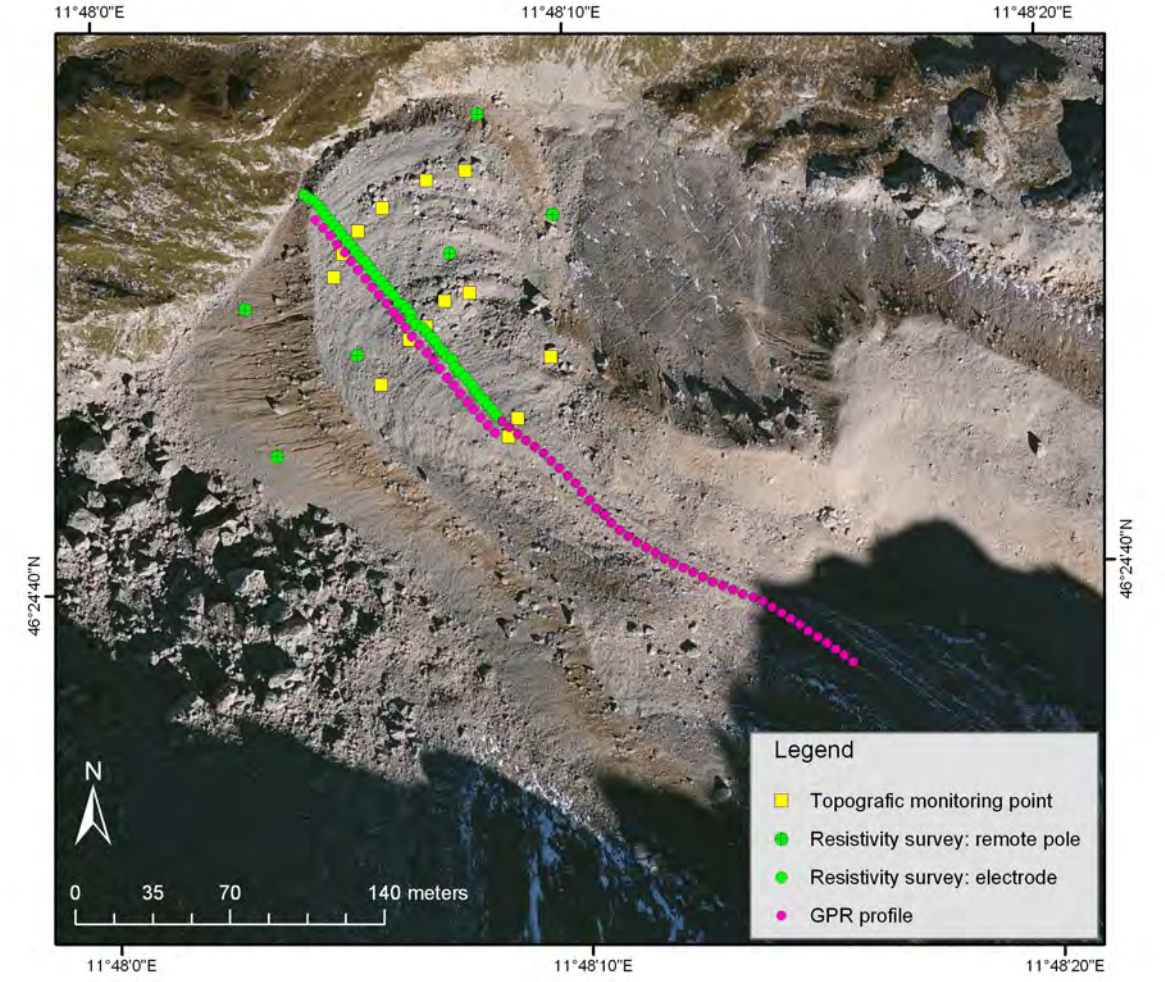


Fig. 8 – Location of topographical and geophysical surveys.

Fig. 9 – Morphology of the rock glacier (left); Total resistivity volume

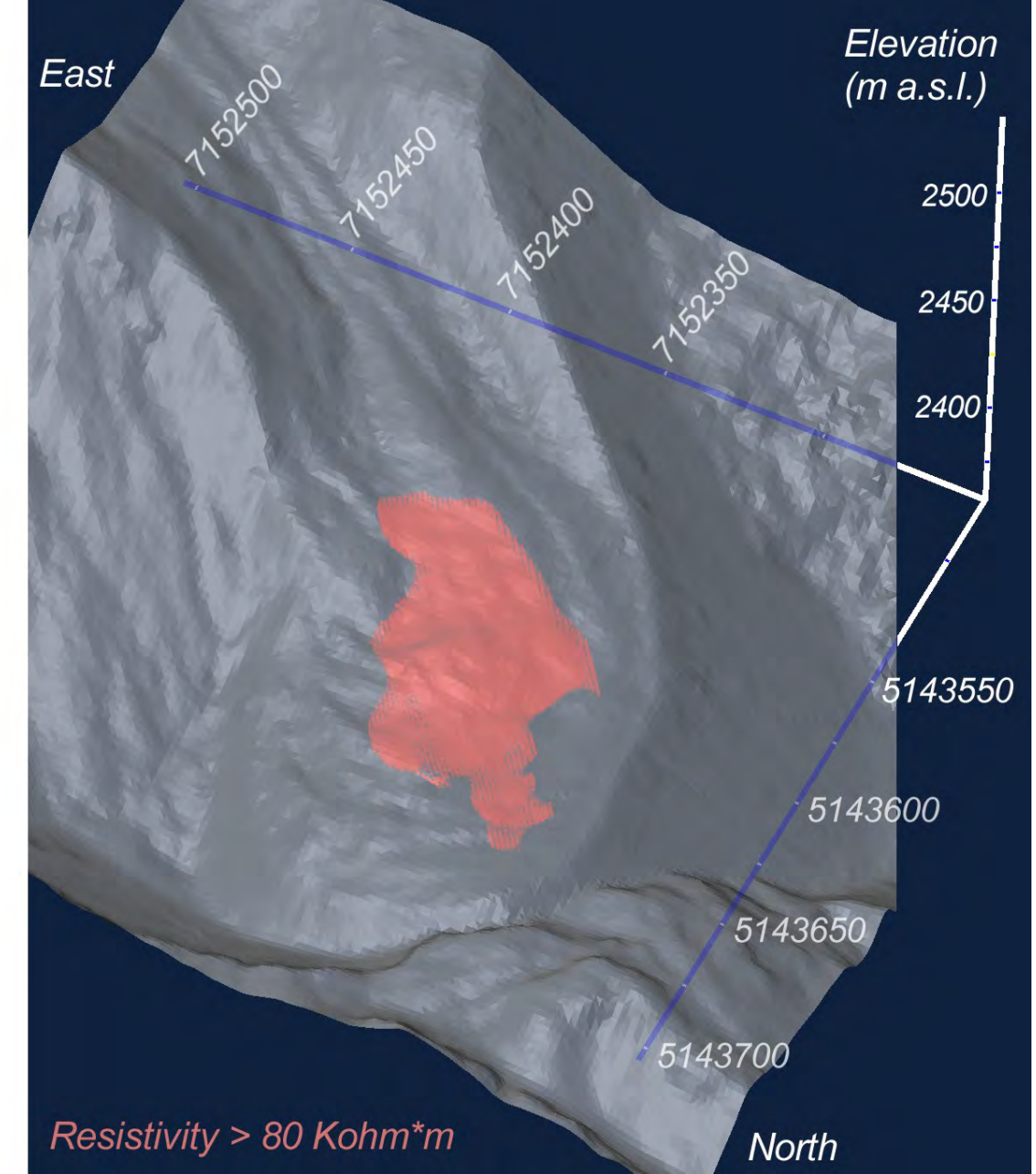
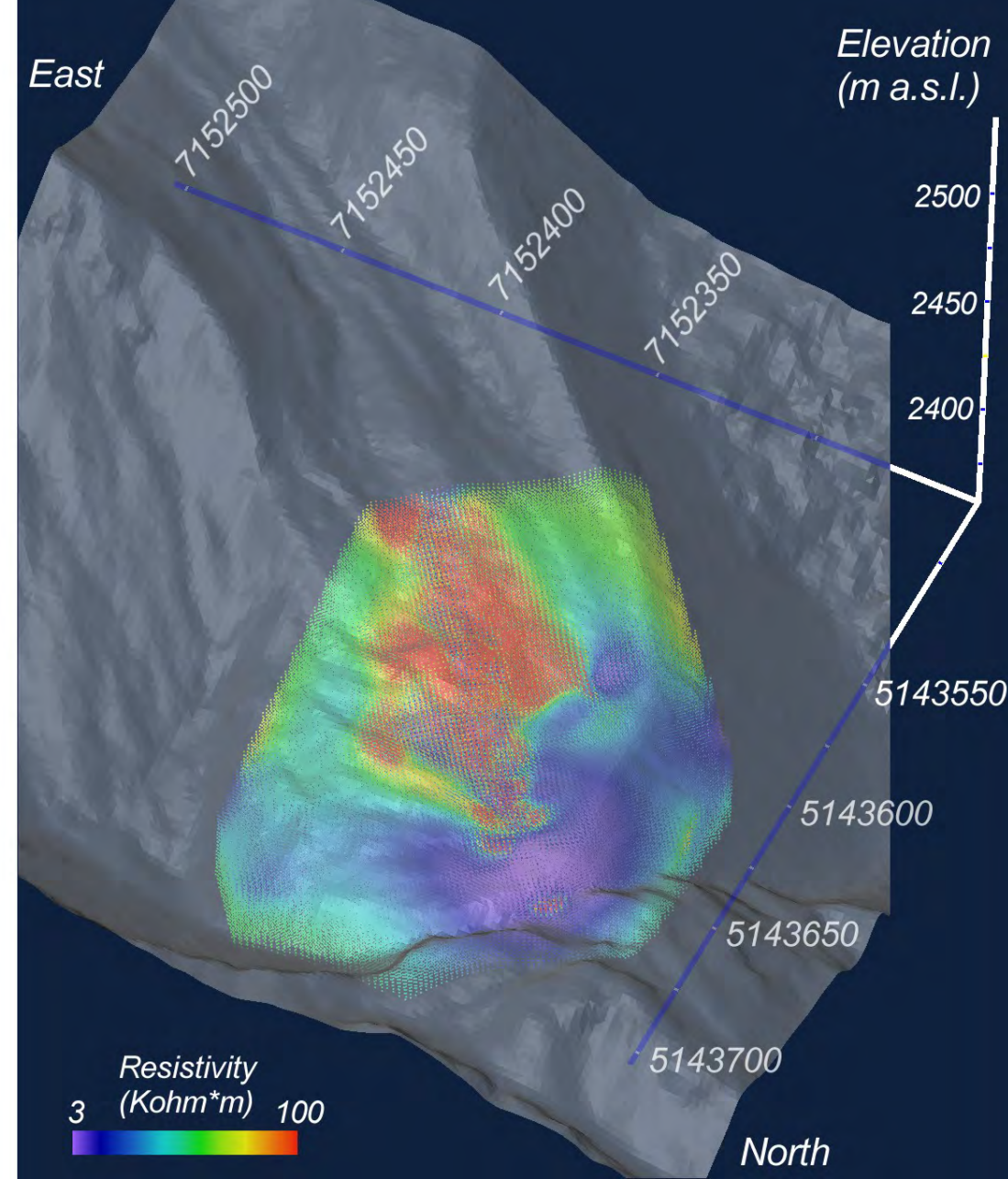
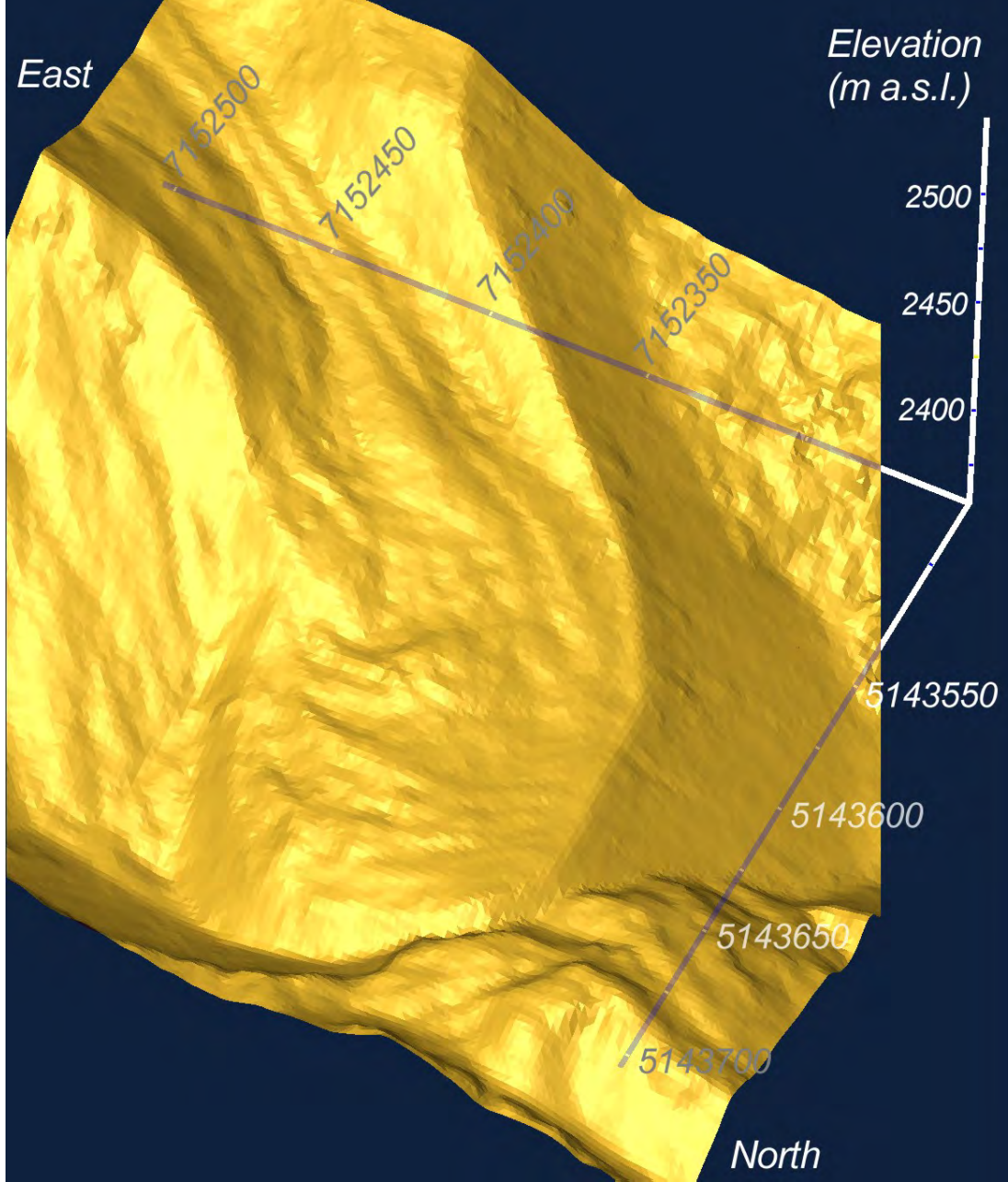


Fig. 10 – GPR Survey.



Fig. 11 – GPR Survey.



Fig. 12 – Transport on site of the equipment by helicopter.

Acknowledgements:

This work has been carried out within the PRIN 2010-2011 project "morphodynamic Effects and environmental impacts of the degradation of the cryosphere in the Eastern Alps" (local head Prof. G. dalla Fontana) and the Agreement between the Geological Survey of the Autonomous Province of Trento, the Department of Geosciences at the University of Padua and the Department of Earth and Environmental Sciences of Pavia for the monitoring of permafrost in Trentino".

References:

Carton A., Meneghel M., Seppi R. (2009) – Il ghiacciaio dell'Uomo (Dolomiti): un esempio di evoluzione da ambiente glaciale a paraglaciale. III National AlGeo Conference 13-18 Settembre 2009 Modena, Alta Badia, 33-34.
Castiglioni B. (1925) – Alcuni ghiacciai nelle Dolomiti e il loro ambiente orografico e climatico. Boll. Club Alpino It., 42 (75), 323-379.
Cossart E., Perrier R., Schwarz M. & Houe S. (2008) – Mapping permafrost at a regional scale: interpolation of field data by GIS application in the Upper Durance catchment (Southern French Alps). GeoFocus 8, 205-224.
Fu P. & P. M. Rich (2002) – A Geometric Solar Radiation Model with Applications in Agriculture and Forestry. Computers and Electronics in Agriculture, 37, 25-35.
Fu P. (2000) – A Geometric Solar Radiation Model with Applications in Landscape Ecology. Ph.D. Thesis, Department of Geography, University of Kansas, Lawrence, Kansas, USA.
Hausmann, H., Krainer, K., Brückl, E., and Mostler, W., 2007: Internal structure, composition and dynamics of Reichenkar rock glacier (western Stubai Alps, Austria). – Permafrost and Periglacial Processes 18: 351-367.
Rich P. M., Dubayah R., Hetrick W. A. & Saving S. C. (1994) – Using Viewshed Models to Calculate Intercepted Solar Radiation: Applications in Ecology. American Society for Photogrammetry and Remote Sensing Technical Papers,